Proposal to Assemble a High Resolution - Electron Sensitive - Energy Flow Calorimeter in the NEULAND Spectrometer

Fermilab, P.O. Box 500, Batavia, IL 60510

Physics Department, Harvard University, Cambridge, MA 02138

Physics Department, Northwestern University, Evanston, IL 60201

Physics Department, Ohio State University, Columbus, OH 43210

Physics Department, University of Pennsylvania, Philadelphia, PA 19174

Physics Department, Rutgers University, New Brunswick, NJ 08903

Physics Department, University of Wisconsin, Madison, WI 53706

(Spokesmen D. D. Reeder and H. H. Williams)

Abstract

We propose to assemble the γ catcher and liquid scintillation calorimeter modules in a simple configuration that is well suited to the investigation of several different neutrino induced processes. We note that the variety of neutrino beams now available at Fermilab and synchrotron intensity and energy together with the high resolution calorimeter allow a multiplicity of experiments to be carried out with a single detector configuration.

Contents

1. Introduction

The discoveries of weak neutral currents,[1] dimuon,[2] μe[3] events and of trimuons[4] in high energy neutrino and antineutrino interactions have caused great excitement in the past few years. These initial observations are now being followed by a period of intense quantitative study of the phenomena. For example the bulk of the dimuon and μe events can now be confidently ascribed to the semileptonic decay of charmed particles. The inclusive weak neutral current cross sections and scaling variable distributions are becoming better understood and a self-consistent value of the Weinberg angle $\sin^2\theta_w$ can be extracted from these data. The trimuon and other multimuon processes are still in a qualitative state of investigation but very likely indicate new physics beyond charm and are probably complicated by several kinds of new physics (e.g., heavy leptons, t and b quarks, etc.).

We propose to assemble a neutrino detector in Lab C capable of performing quantitative measurements of single lepton final states and of the inelastic weak neutral current processes using the available neutrino and antineutrino beams at Fermilab. In addition we believe that a quantitative measurement of the cross section for the processes

$$\nu_\mu e^- \rightarrow \nu_\mu e^-$$

$$\bar{\nu}_\mu e^- \rightarrow \bar{\nu}_\mu e^-$$

can be made with this detector. The study and comparison of multilepton processes such as

$$\nu_\mu + N \rightarrow \mu\mu\mu + X$$
$$\rightarrow \mu\mu e + X$$
$$\rightarrow \mu ee + X$$
$$\rightarrow \mu\mu\mu\mu + X$$
$$\rightarrow \mu\mu ee + X$$
$$\rightarrow \mu\mu\mu e + X$$

will be carried out. The study of these reactions involving both muons and electrons will be important for the understanding of the origin of the multilepton processes.

The proposed detector will enable us:

1) to measure with good resolution the energy of the hadronic cascade by means of a liquid scintillator and lead calorimeter.

2) to identify electrons and photons and to measure their energy and production angle.

3) to measure the direction of the hadronic cascade by the "energy flow" technique.

4) to identify the muons in the final state and measure their momentum and angle, using the muon spectrometer facility.

2. Outline of the New Detector

The new detector will be assembled from existing components as much as possible. The overall plan view of the new detector is shown in Fig. 1. The iron calorimeter and muon spectrometer are essentially unchanged from E-310. We now propose to replace the previous upstream detector by four super modules consisting of optical spark chambers, liquid scintillators, lead-scintillator counters (γ catchers), and arrays of proportional tubes. In Fig. 2 we detail the arrangement of a super module. The characteristics of the various components of the detector are described below.

(I) The large angle muon spectrometer

The design of the 24' magnet system was based on the common characteristic of the kinematic upper limits to the p_μ-θ_μ plots for various values of E_ν. These are shown for E_ν between 35 and 200 GeV in Fig. 3, where it can be seen that for $\theta_\mu \gtrsim 300$ mrad, p_μ is $\lesssim$ 20 GeV, independent of E_ν. Thus for $\theta_\mu \gtrsim 300$ mrad, it is possible to make a satisfactory measurement of p_μ and of the sign of the muon charge with the relatively short magnetic field region (~60 cm per toroid). Above $\theta_\mu \simeq$ 500 mrad, the likelihood that the muons will range out is significant and the thin toroids of the 24' magnet enable a reasonably accurate measurement of the muon momentum by range. As θ_μ decreases, a longer path in the magnetic field is required to measure the larger p_μ, and the 12' magnetic spectrometer provides this additional field. The efficiency for the calorimeter spectrometer combination as a

function of the scaling variables x and y is shown in Fig. 4.

The muon spectrometer consists of three 24' diameter toroids 2' thick and four 12' diameter toroids each about 5' thick. All magnets are driven into saturation. Wide gap spark chambers are used to record the muon tracks in the spectrometer. These chambers have excellent resolution and allow measurement of the muon direction as well as its location. Our experience in the reconstruction of single muon and multimuon events indicates that the direction information is crucial in assigning sparks to tracks. The spectrometer is photographed with both 90^{o} and 15^{o} stereo systems.

(II) Iron-Liquid Scintillator Calorimeter

This component of the apparatus is intended to provide good containment of the hadronic-electromagnetic cascades that originate further upstream in the target-detector. The iron plates provide a convenient, compact way of introducing about 6 nuclear absorption lengths at the end of the target detector. In this calorimeter-absorber the residual energy of a cascade can be measured with acceptable accuracy, as recent studies of iron-plate calorimeters have shown.[5]

(III) Liquid Scintillator-Lead

This calorimeter and the associated wide gap spark chamber are used to measure the hadronic energy, to measure the direction of the hadronic cascade by energy flow, to identify electrons and to measure their energy. The calorimeter resolution will be similar to that of the ElA detector for which the "measured" hadronic resolution is shown in Fig. 5.

The separation of electrons from hadrons is accomplished in the γ catcher-Pb array. Fig. 6 shows the principle of the technique, which depends on the vastly different values of collision length and radiation length.

A prototype of the super module is presently installed upstream of the E310 detector. Early measurements obtained using this prototype will establish the electron energy and angular resolution and the hadron rejection as well as information about the energy flow technique.

HIGH RESOLUTION-ELECTRON SENSITIVE-ENERGY FLOW NEULAND DETECTOR

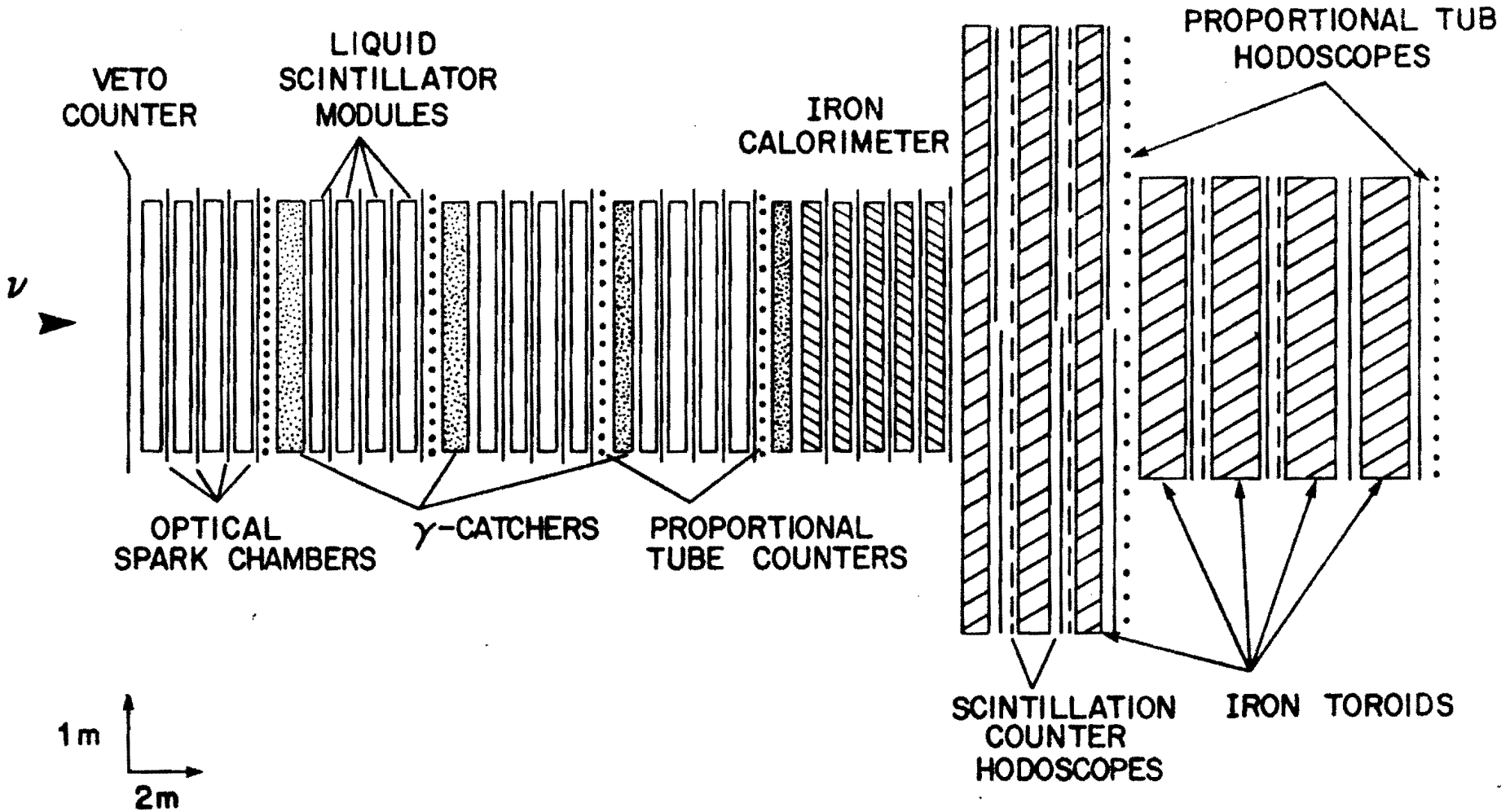

Figure 1

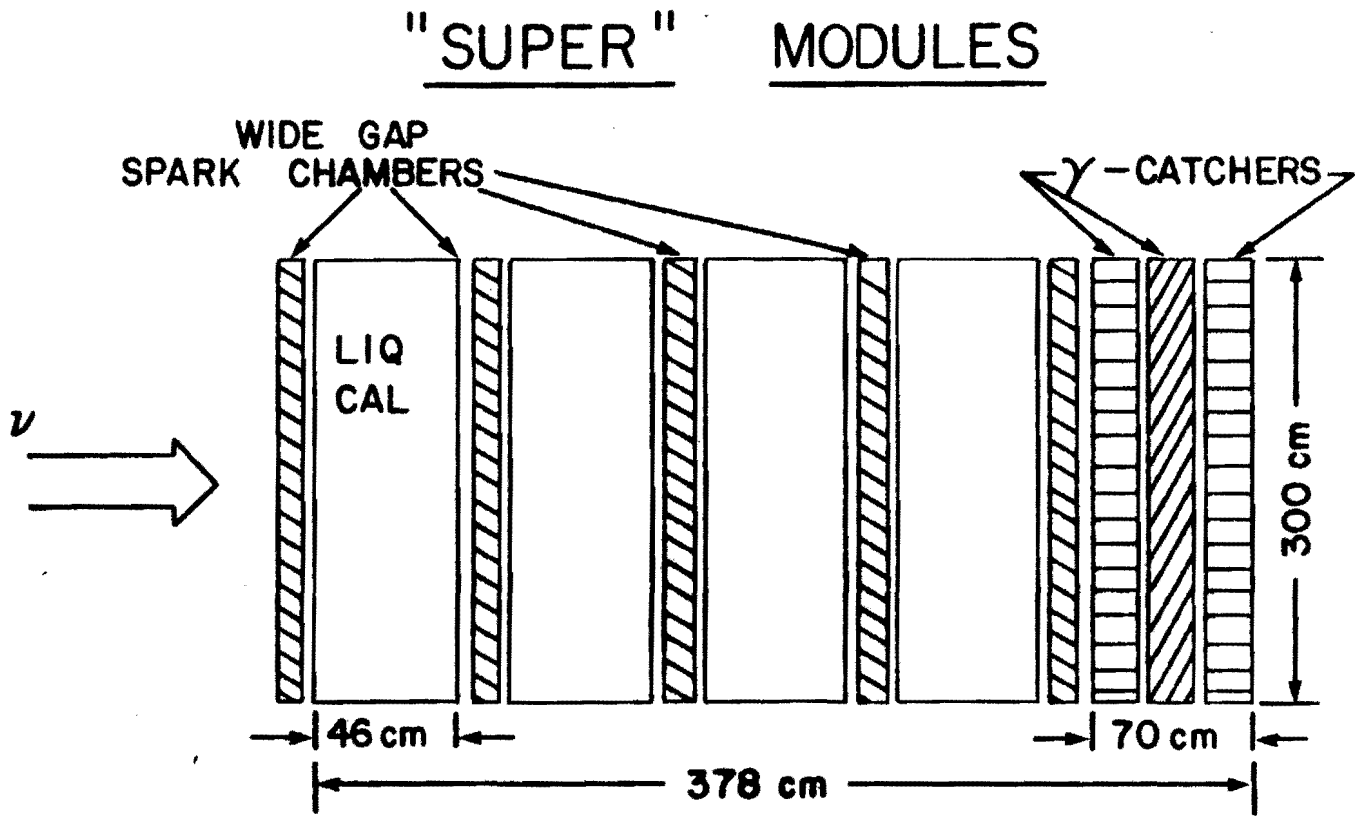
"SUPER" MODULES
WIDE GAP
SPARK CHAMBERS
γ-CATCHERS
LIQ
CAL
ν
300 cm
46 cm
70 cm
378 cm

Figure 2

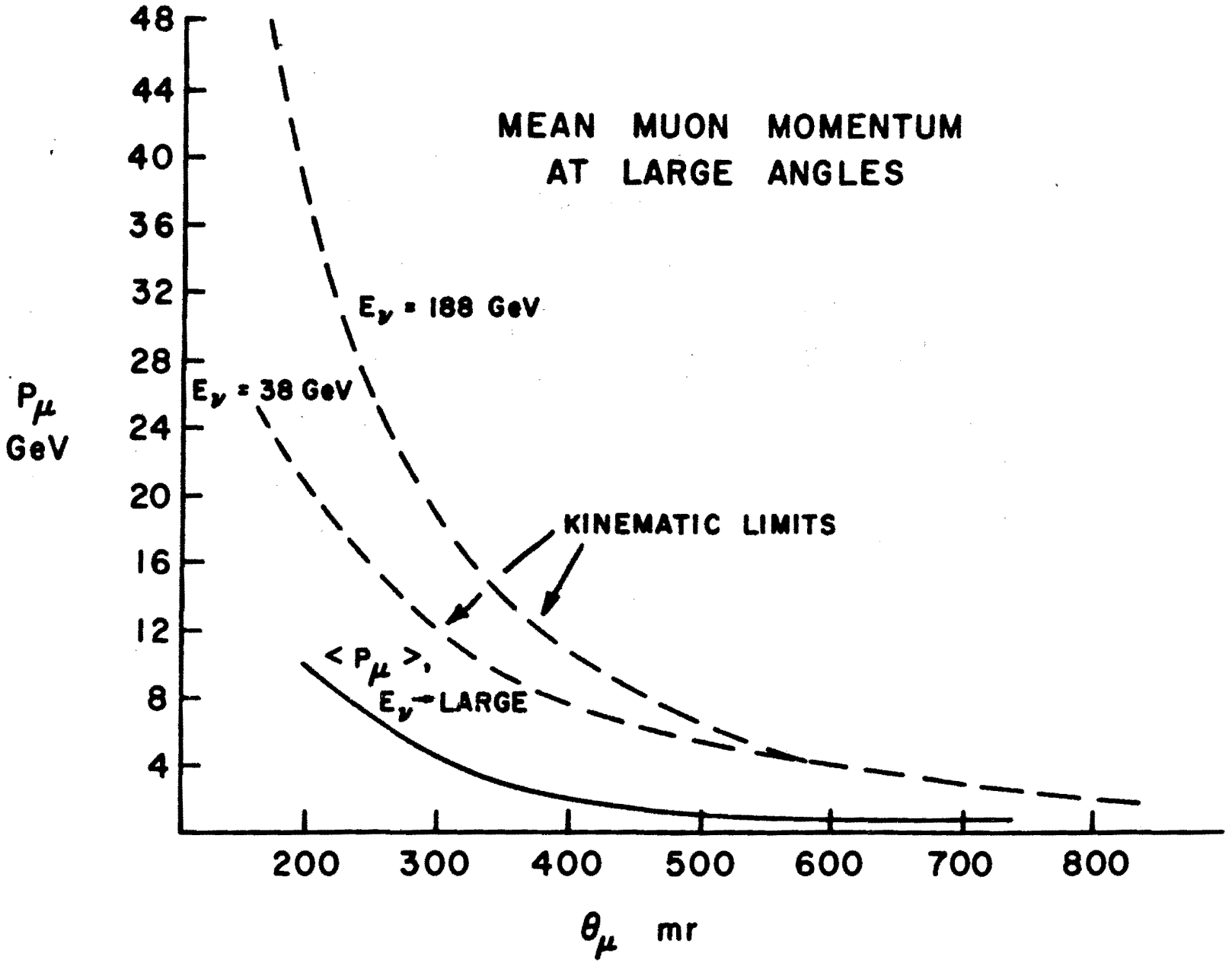
MEAN MUON MOMENTUM
AT LARGE ANGLES
E_ν = 188 GeV
E_ν = 38 GeV
KINEMATIC LIMITS
$\langle P_\mu \rangle$, E_ν → LARGE
P_μ GeV
θ_μ mr
48
44
40
36
32
28
24
20
16
12
8
4
200
300
400
500
600
700
800

Figure 3

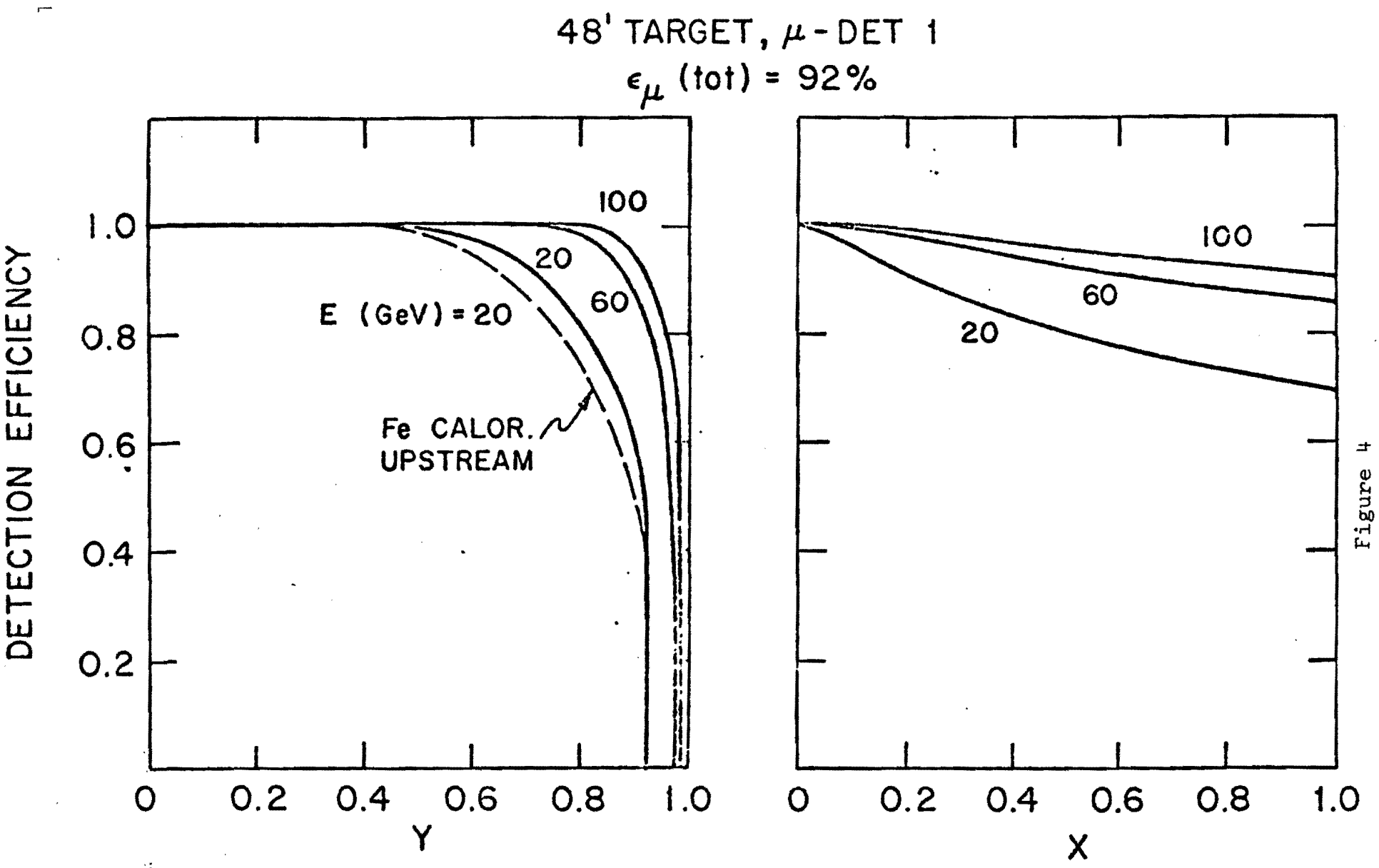
48' TARGET, μ - DET 1
ϵ_μ (tot) = 92%
DETECTION EFFICIENCY
1.0
0.8
0.6
0.4
0.2
0
0.2
0.4
0.6
0.8
1.0
Y
X
100
20
60
E (GeV) = 20
Fe CALOR.
UPSTREAM

Figure 4

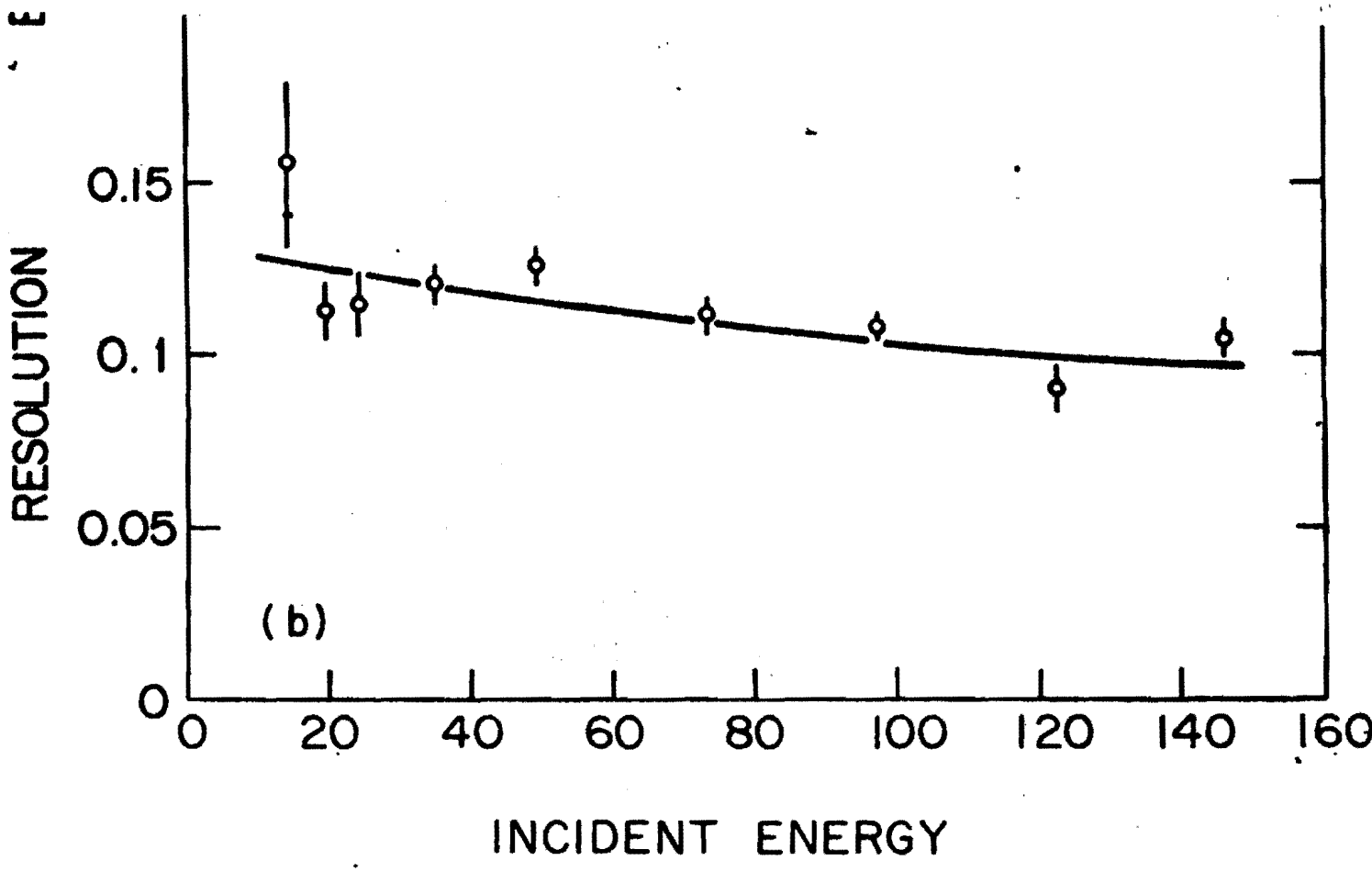

Fig. 10

Figure 5

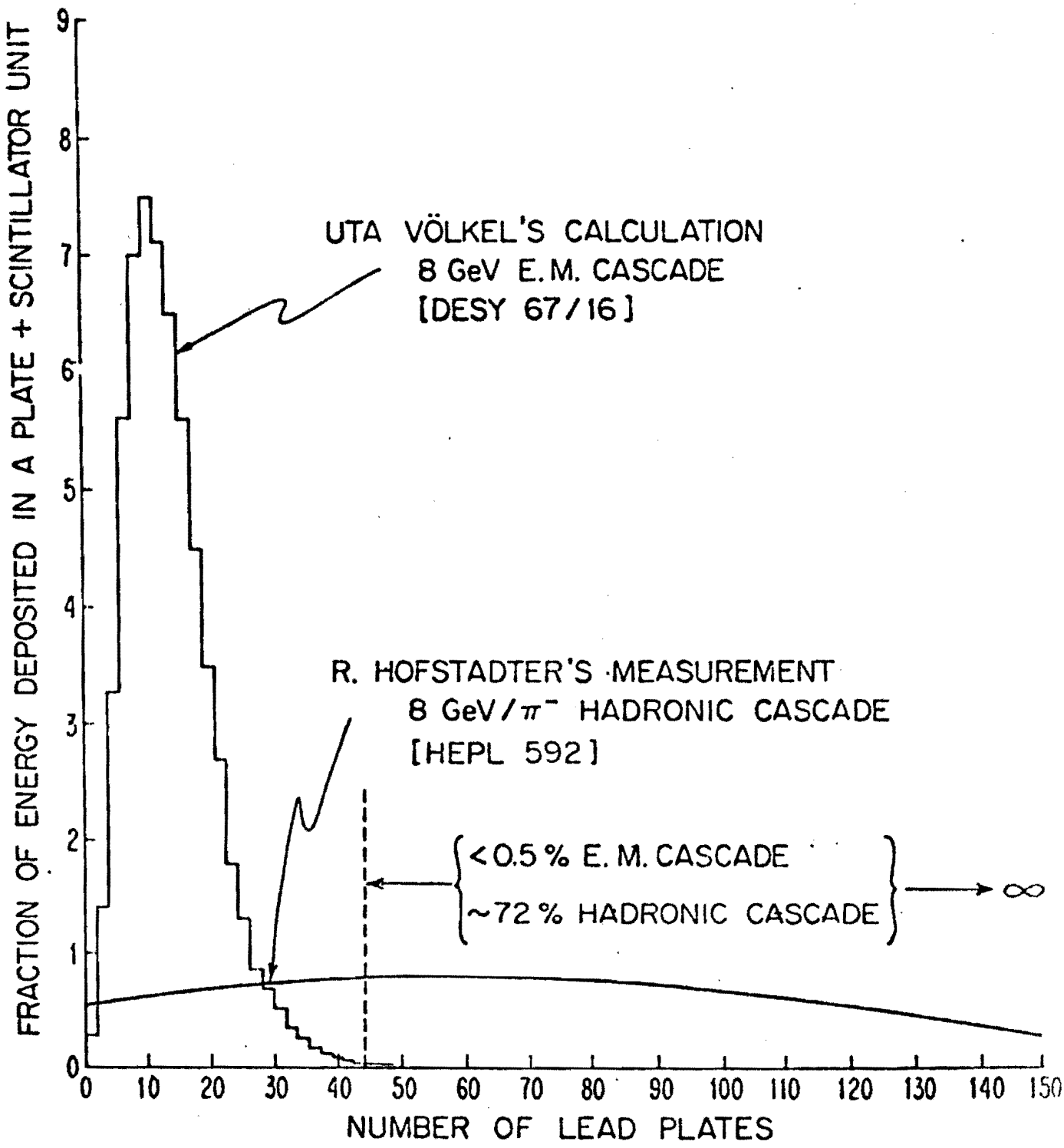
FRACTION OF ENERGY DEPOSITED IN A PLATE + SCINTILLATOR UNIT
NUMBER OF LEAD PLATES
UTA VÖLKEL'S CALCULATION
8 GeV E.M. CASCADE
[DESY 67/16]
R. HOFSTADTER'S MEASUREMENT
8 GeV/π⁻ HADRONIC CASCADE
[HEPL 592]
<0.5 % E. M. CASCADE
~72 % HADRONIC CASCADE
∞

Figure 6

3. The Study of $\nu_\mu(\bar{\nu}_\mu)e^-$ Elastic Scattering Using the Long Spill Horn

The elastic scattering of neutrinos and antineutrinos from electrons

$$\nu_\mu e \rightarrow \nu_\mu e \quad (1)$$

$$\bar{\nu}_\mu e \rightarrow \bar{\nu}_\mu e \quad (2)$$

is of fundamental importance as a probe of the purely leptonic neutral current interaction. Furthermore, interest in these reactions has intensified recently due to the apparent lack of parity violation in atomic physics experiments. This absence of parity violation is inconsistent with simple $SU(2)_L \times U(1)$ gauge models, while virtually all other existing data on semi-leptonic neutral current interactions agree remarkably well with such models. Several theoretical papers "explain" this discrepancy by hypothesizing that the leptonic neutral current is pure vector, at the expense of introducing heavy right-handed leptons or additional intermediate vector bosons. Measurement of the ratio $R_{\nu_\mu e} = \sigma(\bar{\nu}_\mu e \rightarrow \bar{\nu}_\mu e)/\sigma(\nu_\mu e \rightarrow \nu_\mu e)$ will confirm ($R_{\nu_\mu e} = 1$) or reject ($R_{\nu_\mu e} \neq 1$) this conjecture, and in any event will determine the leptonic neutral current coupling.

Since the ratio of cross sections is of prime interest, it is important that the experiment be carried out with a detector in which the systematics of ν_μ and $\bar{\nu}_\mu$ charged current interactions are well understood.

Because the neutrino scatters from an electron target, the center of mass energies and hence cross sections, for reactions 1) and 2) are small, typically 2000 ($\approx M_p/M_e$) times smaller than neutrino-nucleon neutral current interactions. We assume, for simplicity in making rate calculations, that $\sigma(\nu_\mu e \to \nu_\mu e) = \sigma(\bar{\nu}_\mu e \to \bar{\nu}_\mu e) = 1.6 \times 10^{-42} E_\nu \text{ cm}^2/e$. This value is in reasonable agreement with existing experimental data and corresponds to the prediction of the Weinberg-Salam model for $\sin^2\theta_w = 0.25$.

The signature for reactions (1) and (2) is a single recoil electron with mean angle relative to the incident ν direction $\theta_e \simeq \sqrt{\frac{2m_e}{E_\nu}}$. The requirement of a single electron with no other visible tracks should eliminate virtually all background from ν_μ interactions with the exception of $\nu_\mu N \to \nu_\mu N\pi^o$. Events from this latter reaction, and low q^2 events of the type $\nu_e n \to e^- p$ constitute the primary background to the extent that they produce single electromagnetic showers. However, the sharp forward peaking of the electron angular distribution for $\nu_\mu e \to \nu_\mu e$ ($\langle\theta_e\rangle \approx 10$ mr for $E_\nu = 10$ GeV) allows a clean separation from these background processes provided sufficient angular resolution is attained.

Detector

A suitable detector must have large mass and the ability to record single electromagnetic showers with high angular resolution. Liquid scintillator is an ideal target; the low value of Z minimizes multiple scattering thereby allowing accurate measurement of the angle of the primary electron, and

the large critical energy ($E_c \simeq 90$ MeV) implies minimum spread of the shower so that the angle of the shower may also be accurately obtained.

The detector must also have high sensitivity to the presence of additional hadrons both charged and neutral. This is well realized by the configuration shown in Figs. 1 and 2.

There exist 16 target sections each of which is .85 radiation lengths composed of a liquid scintillator counter followed by an optical chamber. The optical chamber is ideal for measuring the angle of the primary electron ($\Delta\theta_e \simeq$ 7-10 mr) and for detecting the existence of any additional charged hadrons. Photons from π^o's will convert in the liquid scintillator and therefore be detected in one of the downstream optical chambers. After every four target sections there exist 2 planes of proportional counters and 3 planes of shower detector. Each shower detector ("γ-catcher") consists of ten 27 cm x 350 cm x 14 r.l. sections which are alternately horizontal and vertical. These counters complete the energy measurement of the shower, and separate hadronic from purely electromagnetic cascades, particularly at the trigger level. The proportional counters aid in event selection and in the measurement of the shower position. We emphasize that all of the apparatus currently exists with the exception of the proportional counters.

Rates

We estimate the rate for $\nu_\mu e \to \nu_\mu e$ ($\bar{\nu}_\mu e \to \bar{\nu}_\mu e$) by extrapolation of observed rates in existing experiments at FNAL using the double horn focussed ν beam. In particular the observed event

rate for $\nu_\mu N \to \mu^- + X$ in the 15' chamber is .75 ± 0.1 ev/15 metric tons/10^{13} protons on target (POT). Assuming a fiducial volume of 50 tons, we then expect 1.25×10^6 $\nu_\mu N \to \mu^- + X$ events/ 50 tons/5×10^{18} POT. The rate for $\nu_\mu e \to \nu_\mu e$ will be lower by $\frac{\sigma(\nu_\mu e \to \nu_\mu e)}{\sigma(\nu_\mu N \to \mu^- + X)} = \frac{1.6 \times 10^{-42} \; E_\nu \, cm^2/e}{7.8 \times 10^{-39} \; E_\nu \, cm^2/N}$ and by the electron/nucleon ratio in the target $\frac{N(e)}{N(\text{nucleon})} = \frac{8}{14} = 0.57$. We therefore expect that 150 $\nu_\mu e \to \nu_\mu e$ events will be produced/50 tons/5×10^{18} POT. A similar calculation yields 100 $\bar{\nu}_\mu e \to \bar{\nu}_\mu e$ events/50 tons/5×10^{18} POT.

Background Reactions

The dominant sources of background are expected to be

$$\nu_e n \to e^- p \qquad (3)$$

$$\text{and} \quad \nu_\mu N \to \nu_\mu N \pi^o .$$

For each reaction, the momentum transfer to the hadrons is limited by form factors characterized by a mass M ≃ 1 GeV; the cross sections are therefore independent of energy for E_ν > 1 GeV, and assume the values

$$\sigma(\nu_e n \to e^- p) \simeq 0.8 \times 10^{-38} \; cm^2 .$$

$$\sigma(\nu_\mu N \to \nu_\mu N \pi^o) \simeq 2. \times 10^{-39} \; cm^2 .$$

The ratio of $\sigma(\nu_\mu e \to \nu_\mu e)$ to the background cross sections then increases linearly with E, which is a major advantage of performing the measurement at Fermilab energies.

Background from $\nu_e n \to e^- p$ is reduced by the ratio of ν_e/ν_μ flux, ~1%, and by the fact that the scattering angle of the electron is typically larger than that for $\nu_\mu e \to \nu_\mu e$ in spite of the relatively low momentum transfer to the proton.

Figure 7 presents the scatter plot of the electron energy versus electron angle for $\nu_\mu e \to \nu_\mu e$. It is seen that separation of events is possible for an angular resolution of 10 mr or less. In Fig. 8 we plot the p distribution which conveniently illustrates in one dimension the separation between signal and background.

A single electron traversing 45 cm of liquid scintillator deposits ~90 MeV. Therefore, ν_e induced events in which the outgoing electron is accompanied by hadrons of $\gtrsim$ 150-200 MeV can be vetoed due to the excess energy in the target calorimeter. This should reduce further the background from high energy ν_e's.

Background from $\nu_\mu N \to \nu N\pi^o$ might appear serious because of the relatively large cross section ratio $\frac{\sigma(\nu_\mu N \to \nu_\mu N\pi^o)}{\sigma(\mu_\nu e \to \nu_\mu e)} \simeq 1300$. However, the dynamics of this reaction, predominantly $\Delta(1232)$ production with a rapid q^2 falloff renders it very unlikely that a high energy photon is produced in the forward direction. A Monte Carlo calculation indicates that ~1 event in 10,000 has a photon lying within 10 mr of the ν beam direction. We believe that this background will be negligible compared to the signal and to the background from $\nu_e n \to e^- p$.

4. The Study of ν_e and $\bar{\nu}_e$ Inelastic Scattering.

The question of muon electron universality has been for some time a topic of great interest to students of the weak interaction. The advent of intense muon neutrino beams has enabled investigations of the deep inelastic scattering of ν_μ by both charged and neutral currents resulting in important insights into the structure of matter. Obviously, the quantitative comparison of the inelastic scattering of ν_e to that of ν_μ will be of great importance in future attempts at building theories of the weak interaction.

The capability of identifying electrons which is inherent in this detector can be used to isolate a sample of ν_e inelastic scattering events. In fact they are a background in the study of neutral weak currents induced by muon neutrinos. About 10% of muonless events are due to $\nu_e(\bar{\nu}_e)$ inelastic scattering. As presented in Table I we can expect to accumulate greater than 5000 ν_e events in an exposure of 3×10^{18} protons on target.

After completion of this qualitative study we expect to intensify our efforts concerning electron neutrinos by using an enriched ν_e beam exemplified by the design made by Mori, Pruss and Stefanski included as Appendix I.

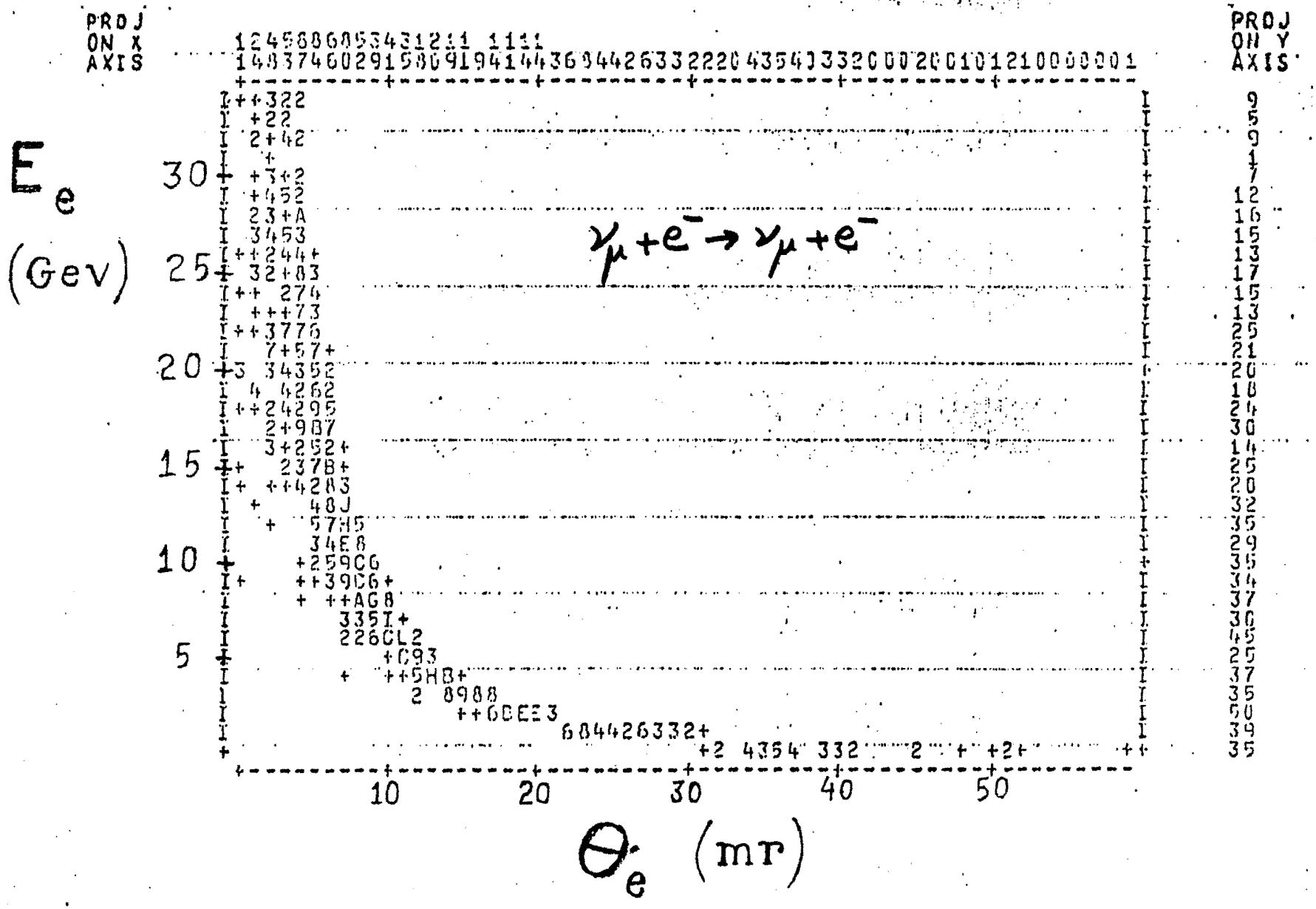
E_e (Gev)
$\nu_\mu + e^- \rightarrow \nu_\mu + e^-$
θ_e (mr)
PROJ ON X AXIS
PROJ ON Y AXIS

Figure 7

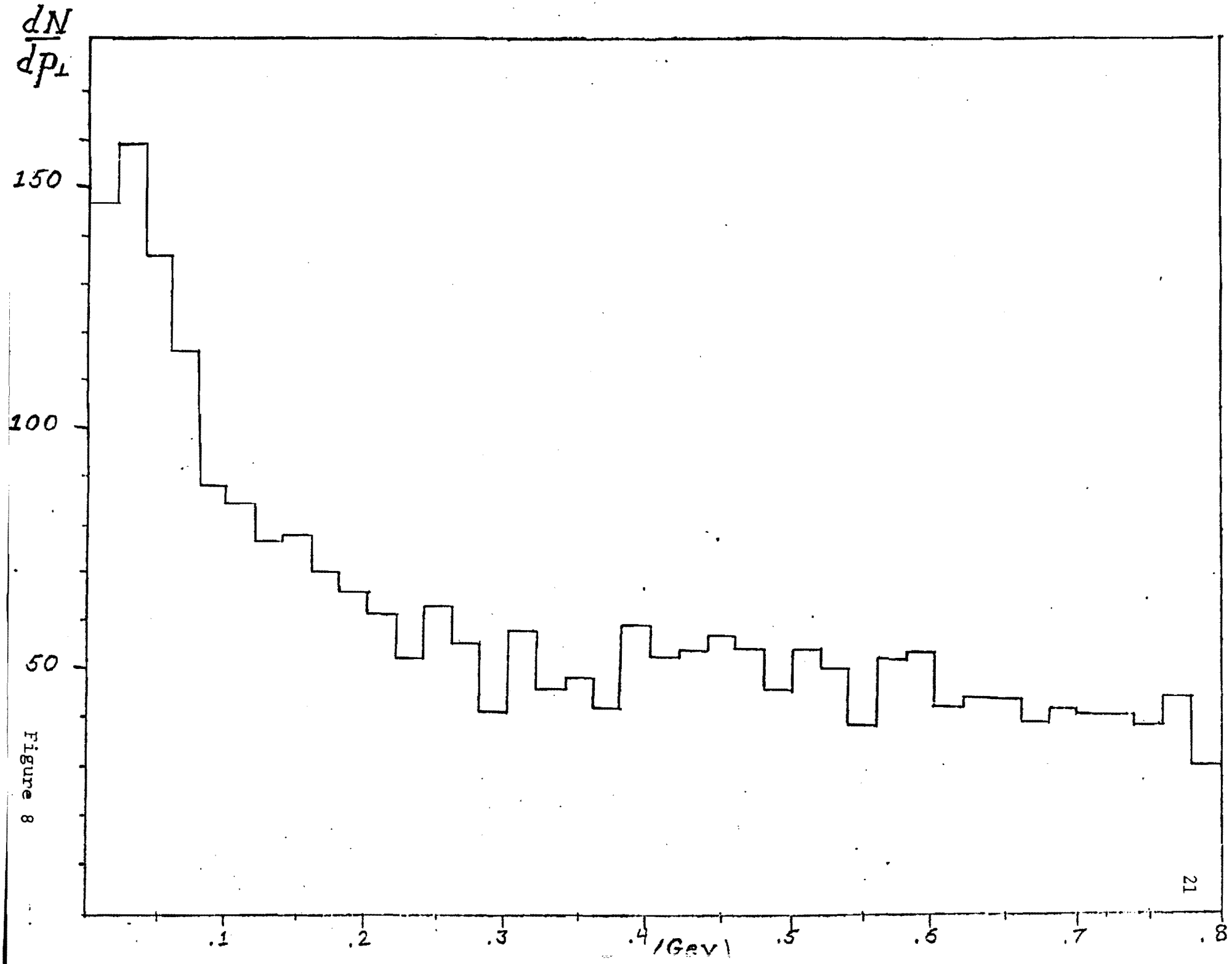

Figure 8

5. Study of Weak Neutral Currents with the Dichromatic Beam

It is clearly of importance to measure as much as possible about the weak neutral current. The proposed detector will very efficiently distinguish the muonless events from the normal charged current interactions. The ability to measure the direction of the hadron shower by means of the energy flow technique when combined with the high resolution energy measurement will permit the study of the weak neutral current throughout the x, y plane.

Certainly, the measurements will be much less precise than equivalent measurements on charged current interactions. The expected angular distribution for the hadronic jet is shown in Fig. 9. Note that the angular distribution has a width in excess of 100 mr. The resolution expected using the energy flow technique is 30-50 mr which is, we believe, adequate to unfold the true distribution.

In order to extract the scaling variable x from the data we first write

$$u = \frac{E_H}{2m_p}\theta_H^2 = x(1 - y)$$

Thus

$$x = \frac{u}{(1-y)} \simeq \frac{E_H^2\theta_H^2}{2m_p[E_\nu - E_H]}$$

The distribution in u calculated using a uniform y distribution is shown in Fig. 10. As $E_H \to E_\nu$ the ratio is extremely poorly defined, which presents a serious problem in extracting the complete x distribution. But away from the y = 1 point a satisfactory measurement is possible.

The calorimeter will provide the first chance to measure other characteristics of the hadron cascade, such as its geometric width and the fraction of primary electromagnetic energy. The comparison to charged current data will be of interest.

The expected rate of events produced by the dichromatic beam within a fiducial volume is presented in Table I. For an exposure of 3×10^{18} protons on target more than 20,000 ν events and 5000 $\bar{\nu}$ neutral current events will be recorded. For a sample this size, systematic errors will dominate the statistical errors.

The experience in analyzing the charged current data obtained in E-310 using the installed supermodules will result in a quantitative determination of the resolution provided by the energy flow technique.

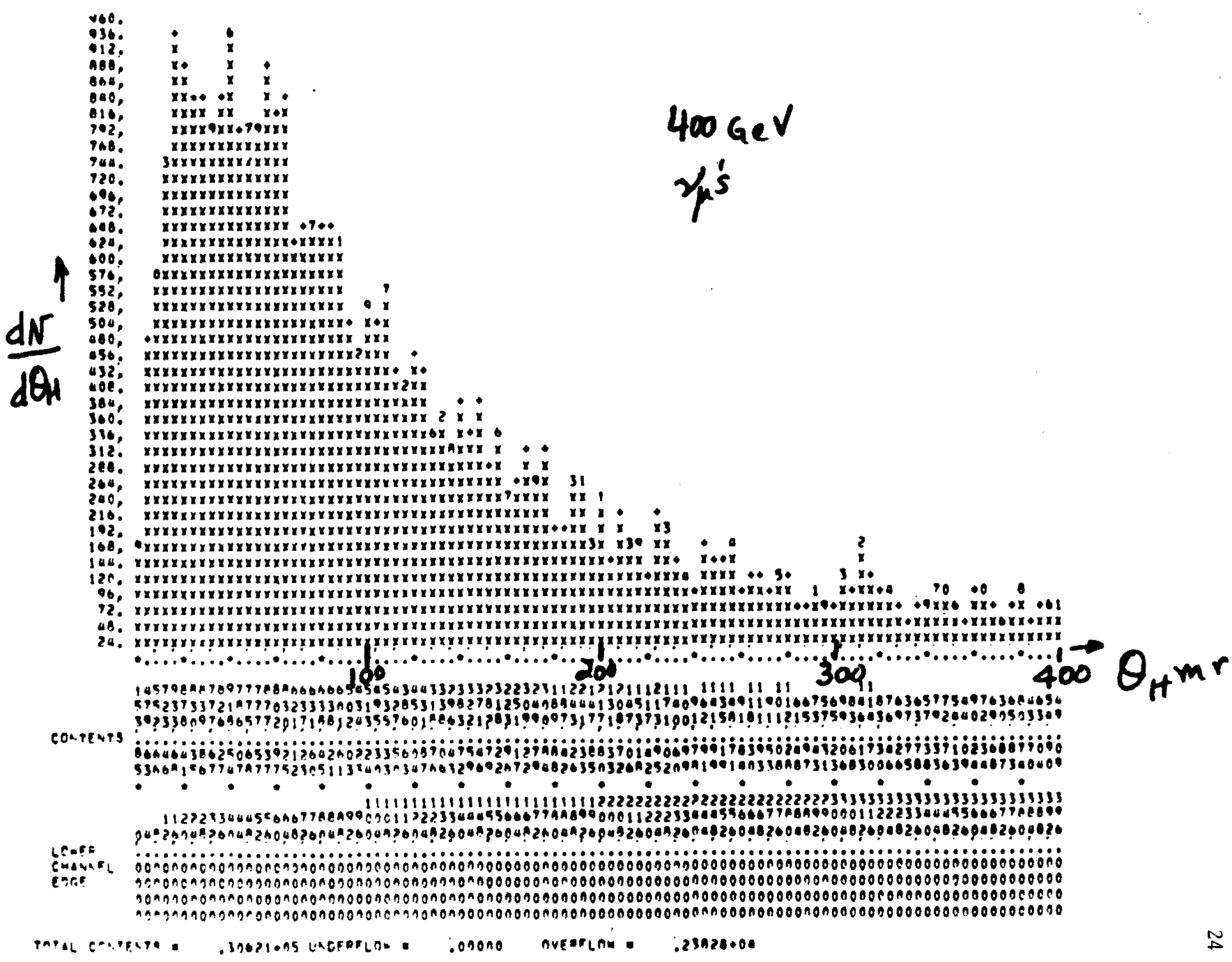
400 GeV
π/μ's
dN/dθH
θH mr
100
200
300
400
CONTENTS
LOWER CHANNEL EDGE
TOTAL CONTENTS = .30621+05 UNDERFLOW = .00000 OVERFLOW = .23828+04

Figure 9

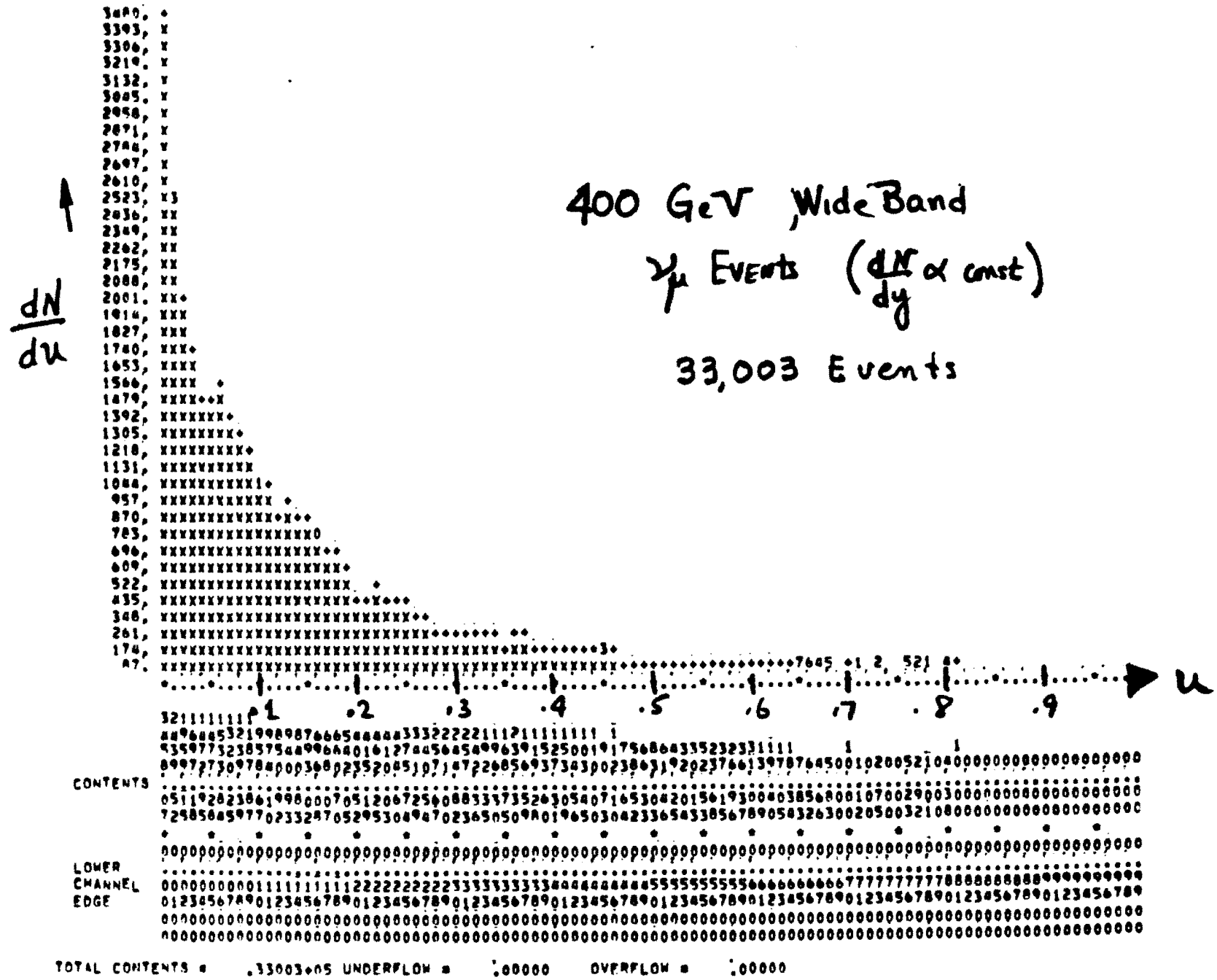
400 GeV, Wide Band
ν_μ Events ($\frac{dN}{dy} \propto$ const)
33,003 Events
$\frac{dN}{du}$
u
CONTENTS
LOWER CHANNEL EDGE
TOTAL CONTENTS = .33003+05 UNDERFLOW = .00000 OVERFLOW = .00000

Figure 10

TABLE I

PROCESSES	CROSS-SECTION (CM^2)	TARGET MASS (Metric Tons)	EVENT RATE PER 10^{17} PROTONS					
			300 GEV 1 HORN	400 Gev 1 HORN	400 GeV 2 HORN	400 GeV QUAD TRIPLET (P_o=125)	400 GeV QUAD TRIPLET (P_o=200)	400 GeV DICHROM (P_o=200)
$\nu_\mu + N \rightarrow \mu^- +$ hadrons	$0.6 \times 10^{-38} E_\nu/N$	162	17,162	29,500	46,470	13,078	6,817	3,061
$\bar{\nu}_\mu + N \rightarrow \mu^+ +$ hadrons	$0.2 \times 10^{-38} E_{\bar{\nu}}/N$	Pb + Liq.	3,885	6,678	10,520	1,763	919	430
$\nu_\mu + N \rightarrow \nu_\mu +$ hadrons	$\sim 0.2 \times 10^{-38} E_\nu/N$	162	6,148	8,850	13,541	3,924	2,046	918
$\bar{\nu}_\mu + N \rightarrow \bar{\nu}_\mu +$ hadrons	$\sim 0.8 \times 10^{-39} E_{\bar{\nu}}/N$	Pb + Liq	460	800	3,500	200	120	160
$\nu_\mu + e^- \rightarrow \nu_\mu + e^-$	$1.4 \times 10^{-42} E_\nu/e^-$	54	0.67	1.15	1.81	0.51	0.27	0.12
$\bar{\nu}_\mu + e^- \rightarrow \bar{\nu}_\mu + e^-$	$4.0 \times 10^{-42} E_{\bar{\nu}}/e^-$	Liq.	1.29	2.23	3.51	0.57	0.30	0.15
$\nu_\mu + Pb \rightarrow \nu_\mu + \mu^+ + \mu^- + Pb$	$5 \times 10^{-41} E_\nu/Pb$	108 Pb	0.46	0.79	1.24	0.35	0.18	0.08
$\nu_\mu + Pb \rightarrow \nu_e + e^+ + \mu^- + Pb$	$7 \times 10^{-41} E_\nu/Pb$		0.64	1.10	1.73	0.49	0.25	0.12
$\nu_\mu + Pb \rightarrow \nu_\mu + e^+ + e^- + Pb$	$10^{-42} E_\nu/Pb$		0.2	0.4	0.6	0.14	0.07	0.03
$\nu_e + N \rightarrow e^- +$ hadrons	$0.6 \times 10^{-38} E_\nu/N$	162	172	295	465	131	68	31
$\bar{\nu}_e + N \rightarrow e^+ +$ hadrons	$0.2 \times 10^{-38} E_\nu/N$	Pb + Liq.	8.6	14.8	23.4	6.6	3.4	1.5
$\nu_e + e^- \rightarrow \nu_e + e^-$	$54. \times 10^{-42} E_\nu/e^-$	54 Liq.	0.03	0.05	0.08	0.02	0.01	0.005

1. Fiducial region in x, y is taken to be 2.8×2.8 m^2

6. Observation of μμe, μee and μμμe Events and Study of μμμ Events

Some important properties of the trimuon events which have been identified in the E-310 analysis are:

1. The large majority of the events are $\mu^-\mu^-\mu^+$.
2. Several events have relatively large (+-) dimuon masses and large $P_\perp$'s.
3. For almost all the events the μ^+ has an energy intermediate between the μ^- energies.
4. Several events have unusually high visible energy and very energetic muons (events 119, 146 and 281). Event 281 is shown in Fig. 11.
5. Several of the events have one or more <u>low</u> energy muons.

These properties suggest that trivial explanations such as π/K decay cannot explain the majority of the trimuon events and that μ pair production at the hadronic vertex or charm pair production will not explain <u>all</u> of the trimuon events. Thus it may be that additional processes are occuring. Nevertheless it is also probable that charm pair production will account for some events. Thus, since several processes may contribute, it will be necessary to collect many tri-lepton events of different kinds in order to understand their physical origin.

One particularly interesting trimuon event is shown in Fig. 12 where all three muons are high energy. The observation of μμe and μee events of comparable energies would be spectacular.

In Fig. 13 is plotted the momentum of the three muons transverse to the neutrino direction, for events 119-17991 and 281-147196. If we assume that one of the two μ^- come from a $\nu_\mu \rightarrow \mu$ vertex and a resulting deep inelastic neutrino collision, then the recoiling hadronic system must balance the P_x and P_y of the leading μ^-. This vector is denoted as H_2 or H_3 for the two possible choices of leading μ^- track in Fig. 10. For either choice the angle between the hadronic recoil vector and the other two muon vectors is constructed and shown in Fig. 10. Note that in nearly all cases the resultant angle is greater than 90°, which is untypical of particles originating from the hadronic vertex. Thus these events are qualitatively characterized as being more "lepton-like" rather than hadron-like.

We are unable to account for these events except to suggest that several processes may be necessary to describe trimuon production. For the most energetic events the three muons appear to cluster on one side of a plane passing through the neutrino beam line, which appears to indicate a physical origin for the additional muons different from the hadronic vertex.

We estimate that an exposure of 5×10^{18} protons on target will yield about 30 μμμ, and comparable numbers of μμe and μee. The sensitivity to the detection of four lepton events will be increased about an order of magnitude.

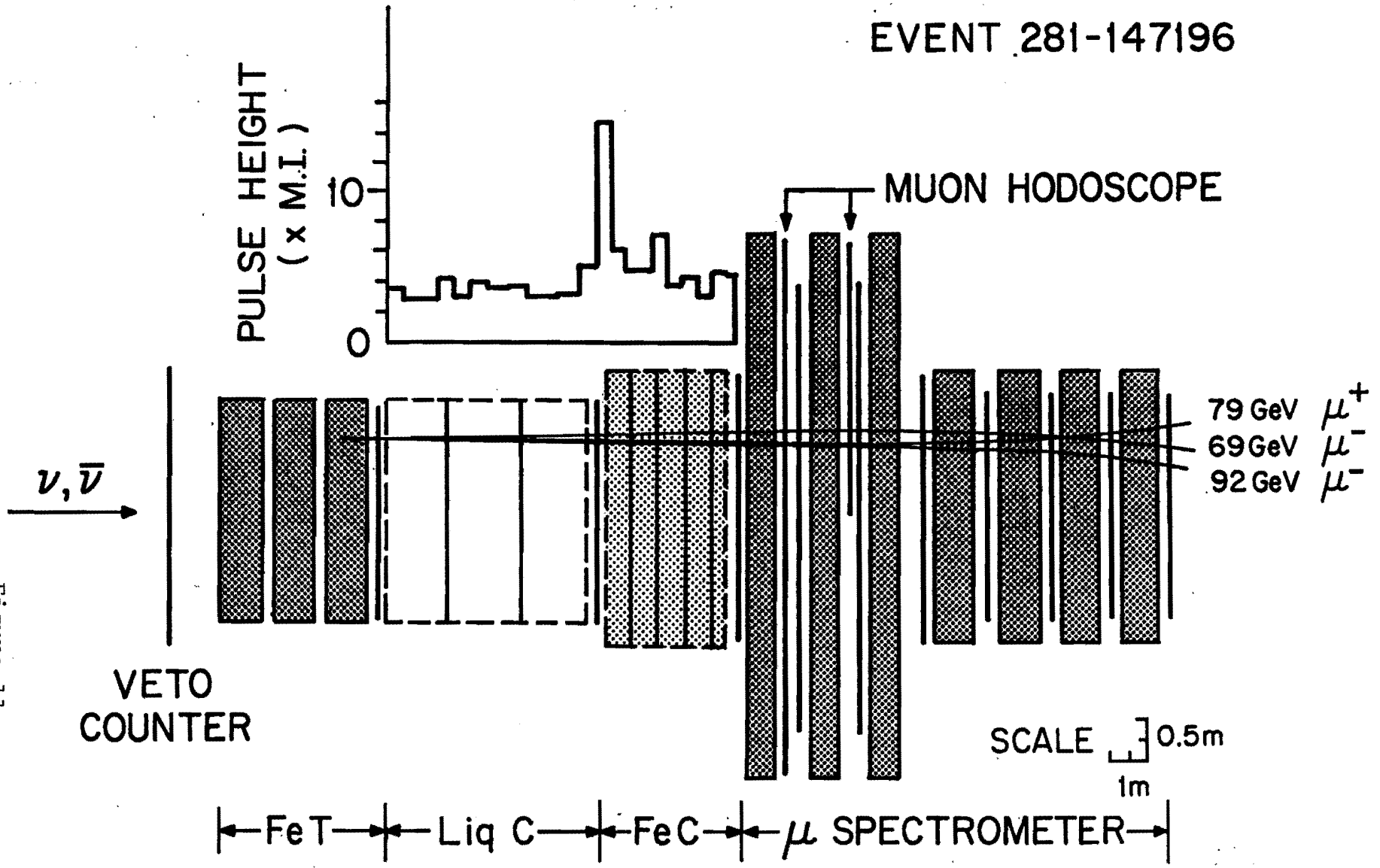
EVENT 281-147196
PULSE HEIGHT
(x M.I.)
10
0
MUON HODOSCOPE
79 GeV μ^+
69 GeV μ^-
92 GeV μ^-
$\nu, \bar{\nu}$
VETO
COUNTER
SCALE
0.5m
1m
FeT
Liq C
FeC
μ SPECTROMETER

Figure 11

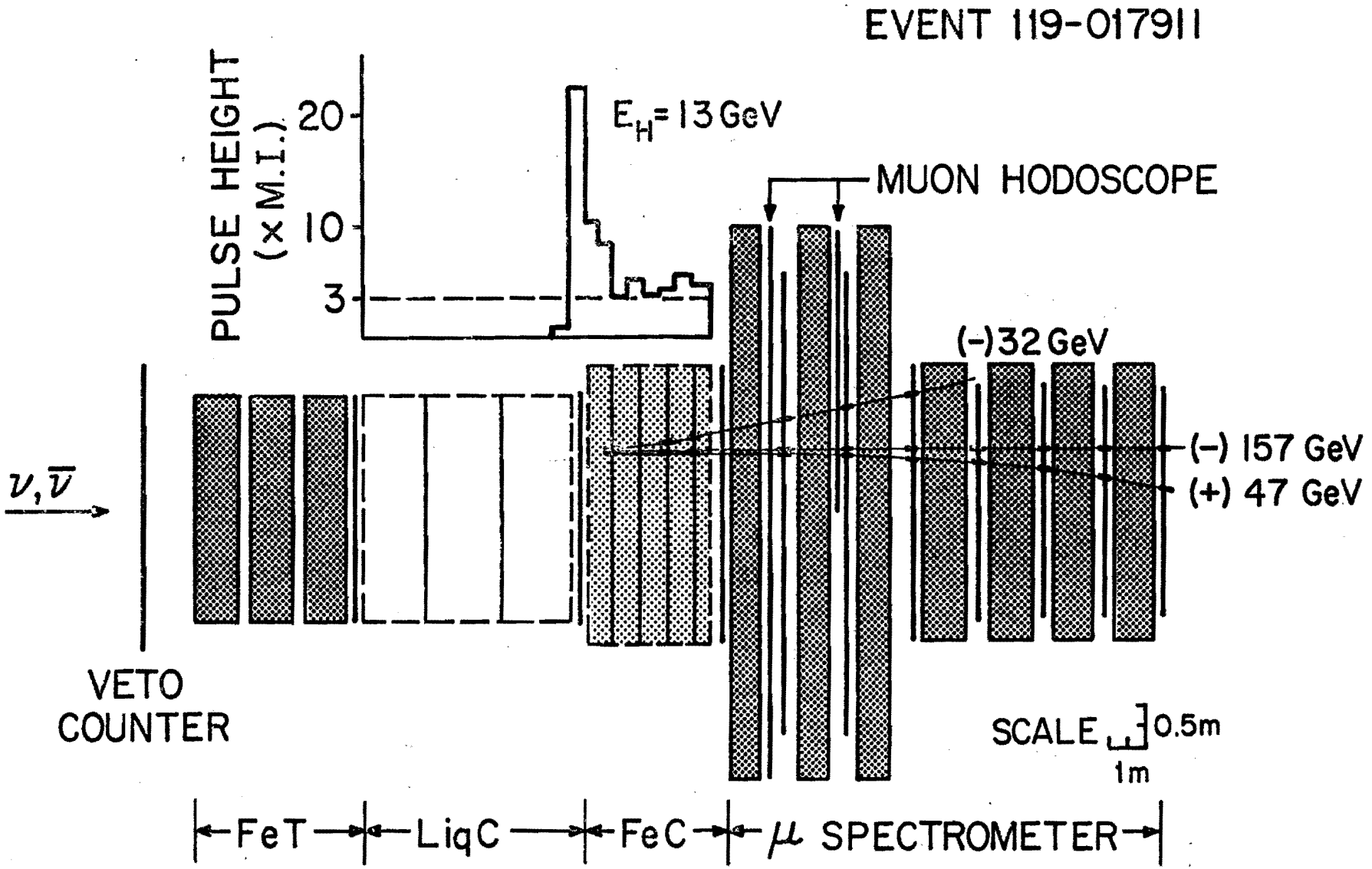
EVENT 119-017911
PULSE HEIGHT (× M.I.)
20
10
3
E_H = 13 GeV
MUON HODOSCOPE
(-)32 GeV
(-) 157 GeV
(+) 47 GeV
$\nu, \bar{\nu}$
VETO COUNTER
SCALE 0.5m
1m
FeT
LiqC
FeC
μ SPECTROMETER

Figure 12

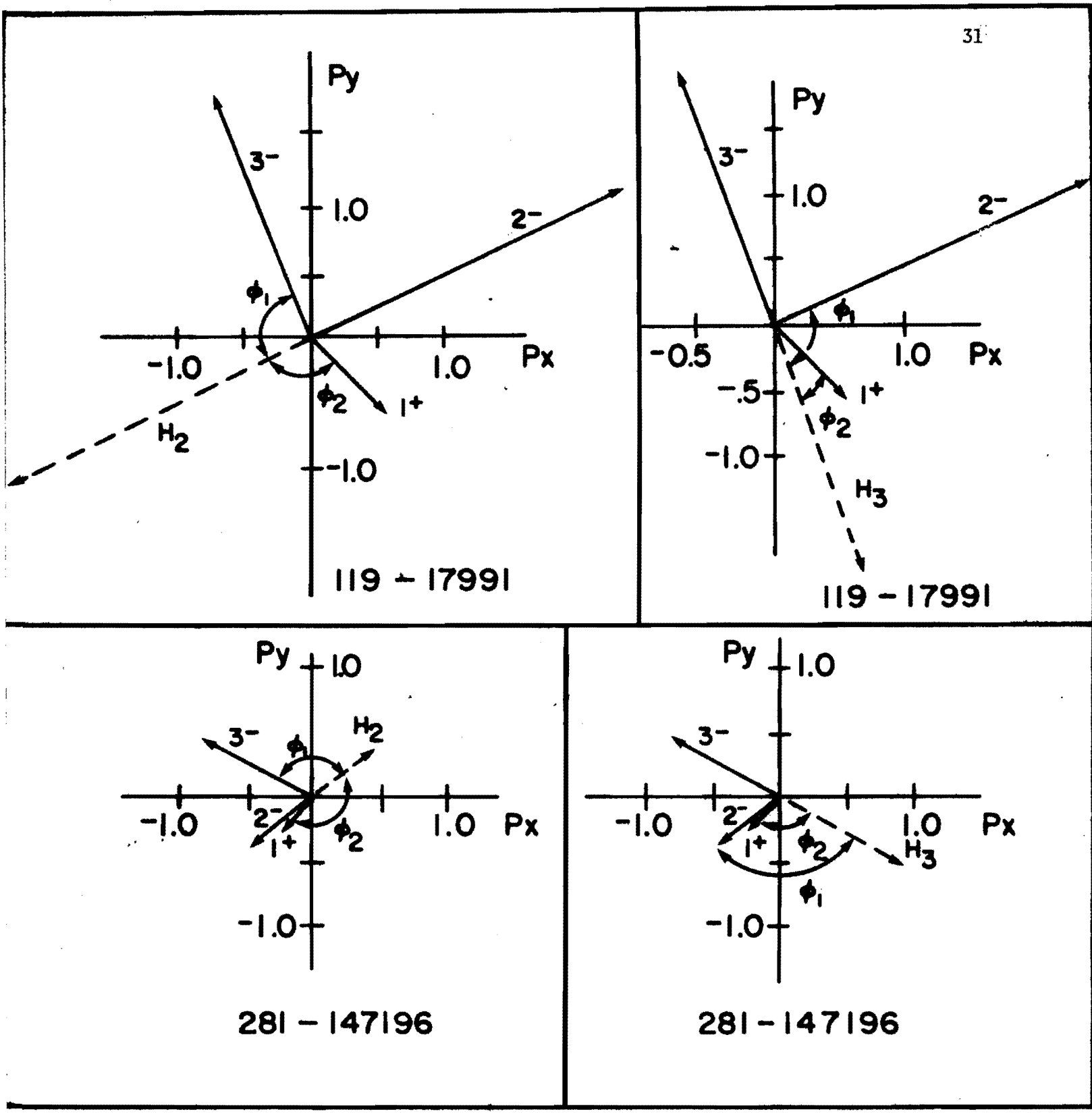
Py
3⁻
1.0
2⁻
ϕ_1
-1.0
1.0
Px
ϕ_2
1⁺
H_2
-1.0
119 - 17991
Py
3⁻
1.0
2⁻
ϕ_1
-0.5
1.0
Px
-.5
1⁺
ϕ_2
-1.0
H_3
119 - 17991
Py
1.0
3⁻
H_2
ϕ_1
-1.0
2⁻
1⁺
ϕ_2
1.0
Px
-1.0
281 - 147196
Py
1.0
3⁻
-1.0
2⁻
1⁺
ϕ_2
1.0
Px
H_3
ϕ_1
-1.0
281 - 147196

Figure 13

7. Specific Request for Beam Time.

This experiment is designed for an intensive study of specific problems in neutrino physics in contrast to the exploratory nature of earlier experiments. Thus it will require new beams and higher intensities than those used in earlier experiments. The continuing upgrading of the facilities and performance of the synchrotron and the neutrino target area are now well matched to this type of intensive inventigation.

We specifically request:

i) $> 3 \times 10^{18}$ protons on the target of the dichromatic beam (ν)
$> 3 \times 10^{18}$ protons on the target of the dichromatic beam ($\bar{\nu}$)
This exposure will be used for detailed study of weak neutral and charged current processes.

ii) 1×10^{19} protons on the target of the long spill double horn (ν)
1×10^{19} protons on the target of the long spill double horn ($\bar{\nu}$)
with plug.

This phase of the experiment will concentrage on muon-neutrino elastic scattering on electrons; multilepton production; electron neutrino scattering; etc.

8. An Investigation of Neutrino Interactions using an Electron Sensitive High Resolution Calorimeter with the FNAL Spectrometer.

Spokesmen - D. D. Reeder and H. H. Williams
Fermilab, Northwestern, Ohio State, Harvard, Pennsylvania, Rutgers, and Wisconsin collaboration.

The FNAL neutrino detector is to be reconstructed using liquid scintillator tanks and lead-scintillator counters (γ catchers) together with optical spark chambers and proportional tube counters arranged as four super modules. This detector is to be installed in front of the thick plate calorimeter and muon spectrometer used in E-310. This detector is optimized to identify electrons and to measure their energy; to measure the direction and energy of hadron cascades using the "energy flow" technique; and to study multi-lepton final states in great detail.

i) to study the reactions $\nu_\mu(\bar{\nu}_\mu) + N \rightarrow \nu_\mu(\bar{\nu}_\mu) + X$ in the FNAL dichromatic beam. About 3×10^{18} protons on target for both ν and $\bar{\nu}$ will provide a sample well matched to systematic errors.

ii) to study the reaction $\nu_\mu(\bar{\nu}_\mu) + e^- \rightarrow \nu_\mu(\bar{\nu}_\mu) + e^-$ in the FNAL slow spill double horn focussed beam. About 10^{19} protons on target for both ν and $\bar{\nu}$ will be necessary to adequately investigate this important reaction.

iii) to study in detail the multi-lepton final states ($\mu\mu\mu$, $\mu\mu e$, μee, $\mu\mu$, μe, etc.) produced in the beams described above.

The single muon charged current reactions will be studied in part to learn the systematic errors characteristic of the apparatus and to use as normalization for cross section measurements. The ν_e inclusive charged current scattering will also be investigated in the same exposures.

References

1. G. Myatt, in Proceedings of the Sixth International Symposium on Electron and Photon Interactions at High Energies, Bonn, 1973, edited by H. Rollnik and W. Pfeil (North-Holland, Amsterdan, 1974), p. 389; F. J. Hasert et al., Phys. Lett. 46B, 138 (1973); A. Benvenuti et al., Phys. Rev. Lett. 32,

2. B. Aubert et al., "Experimental Observation of $\mu^+\mu^-$ Pairs Produced by Very High Energy Neutrinos", in Proceedings of the Seventeenth International Conference on High Energy Physics, London, 1974 and in Neutrinos - 1974, AIP Conference Proceedings No. 22, edited by C. Baltay (American Institute of Physics, New York, 1974), p. 201. A. Benvenuti et al., Phys. Rev. Lett. 34, 419 (1975), ibid. 34, 597 (1975).

3. J. Blietschau et al., Phys. Lett. 60B, 207 (1976; J. von Krogh et al., Phys. Rev. Lett. 38, 710 (1976).

4. A. Benvenuti et al., Phys. Rev. Lett. 38, 1110 (1977), A. Benvenuti et al., ibid, 38, 1183, B. C. Barish et al., ibid. 38, 577.

ELECTRON NEUTRINO BEAM

S. Mori, S. Pruss and R. Stefanski

April 9, 1977

The Sign Selected Bare Target[1] (SSBT) train can easily be modified for an electron neutrino beam[2]. Figures 1(a) and (b) give schematic layouts of the two arrangements. A modification required for the electron beam is a new beam dump further downstream of the second bending magnet. It might preclude the present beam switching operation between the N7 Beam Line and the N2 manhole target beam. The present beam dump for the SSBT and the second bending magnet can remotely be positioned to either beam.

Figure 2 shows a calculated electron neutrino or anti-neutrino flux from the $K_L^o \to \pi^- e^+ \nu_e$ (or $\pi^+ e^- \bar{\nu}_e$) decay by a Monte Carlo program. The incident proton energy is 400 GeV. The K_L^o cross section is assumed to be the average K^+ and K^- cross sections. Stefanski-White parameterization[3] was used. The muon neutrino background from the π^+ and K^+ decays is also shown. The muon anti-neutrino background from the π^- and K^- decays is substantially smaller than the muon neutrino background. Also shown are the anti-neutrino fluxes for the SSBT and the Triplet Train[4] and the neutrino flux for the Triplet Train. The fluxes for the Triplet Train were computed by the NUADA program[5]. The two anti-neutrino flux curves for the SSBT were computed by the Monte Carlo program and the NUADA program for

comparison. The muon neutrino or anti-neutrino flux from the $K_L^o \to \pi^- \mu^+ \nu_\mu$ (or $\pi^+ \mu^- \bar{\nu}_\mu$) is 70% of the electron neutrino or anti-neutrino flux from the K_L^o decay. The muon neutrino or anti-neutrino backgrounds from pion decays of the $K_S^o \to \pi^+ \pi^-$ are estimated to be relatively small in the present arrangement[6].

One or two magnets can be added to reduce the muon backgrounds originated from the other sources than the K_L^o decay. Other types of magnets might be needed for a cleaner beam and for a reliable and clean beam dump.

Computed electron neutrino fluxes for the present electron neutrino beams are shown in Figure 3 for the incident proton energies of 400, 500 and 1000 GeV. Although at the higher energies longer and high field magnets are required in order to suppress the muon neutrino background from the π^+ and K^+ decays and to achieve reliable beam dump, it seems to be a trivial modification to maintain a similar angular acceptance as the present beam.

REFERENCES

1. R. Stefanski and H. White, Jr., TM626A, 1976.

2. Recent studies about electron neutrino beams are discussed by C. Baltay, et al, in the 1976 Summer Study (Vol. 2, p. 43).

3. R. Stefanski and H. White, Jr., FN292, 1976.

4. A. Skuja, R. Stefanski and A. Windelborn, TM469.

5. D. Carey and V. A. White, Fermilab Internal Report, NUADA, June, 1975.

6. B. Roe, private communication.

FIGURE CAPTIONS

Figure 1(a) Schematic layout for the Sign Selected Bare Target Train

(b) Schematic layout for the electron neutrino beam

Figure 2 Electron neutrino or anti-neutrino flux from the K_L° decay and muon neutrino background from the π^+ and K^+ decays for the present electron neutrino beam. Also are shown muon anti-neutrino flux for the SSBT and anti-neutrino and muon neutrino flux for the Triplet Train configuration used in the run of December, 1976. Two muon anti-neutrino flux curves for the SSBT were computed by the Monte Carlo program and the NUADA program.

Figure 3 Electron neutrino fluxes from the K_L° decay for the incident proton energies of 400, 500 and 1000 GeV.

(A) SIGN SELECTED BARE TARGET

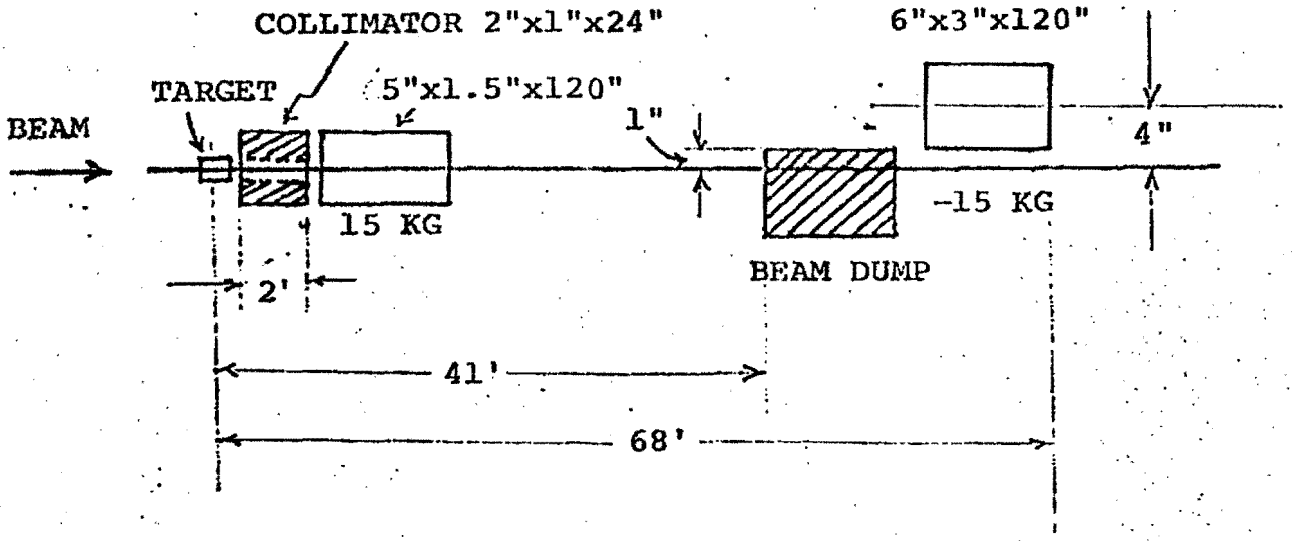

(B) ELECTRON NEUTRINO BEAM

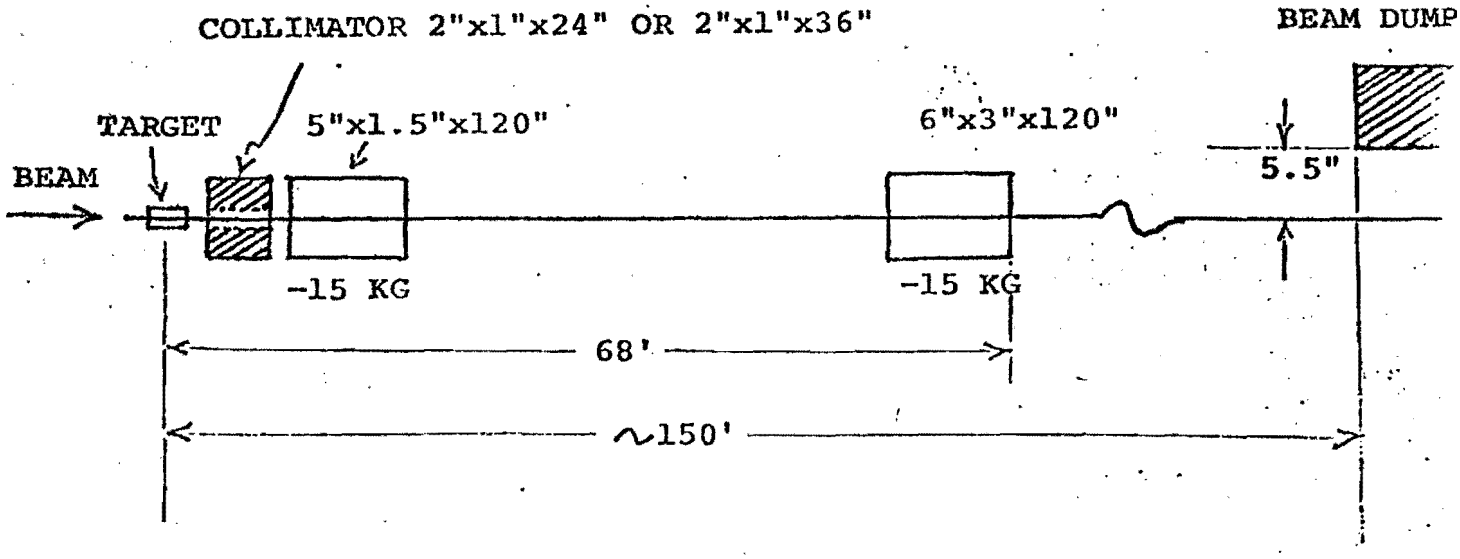

Figure 1.

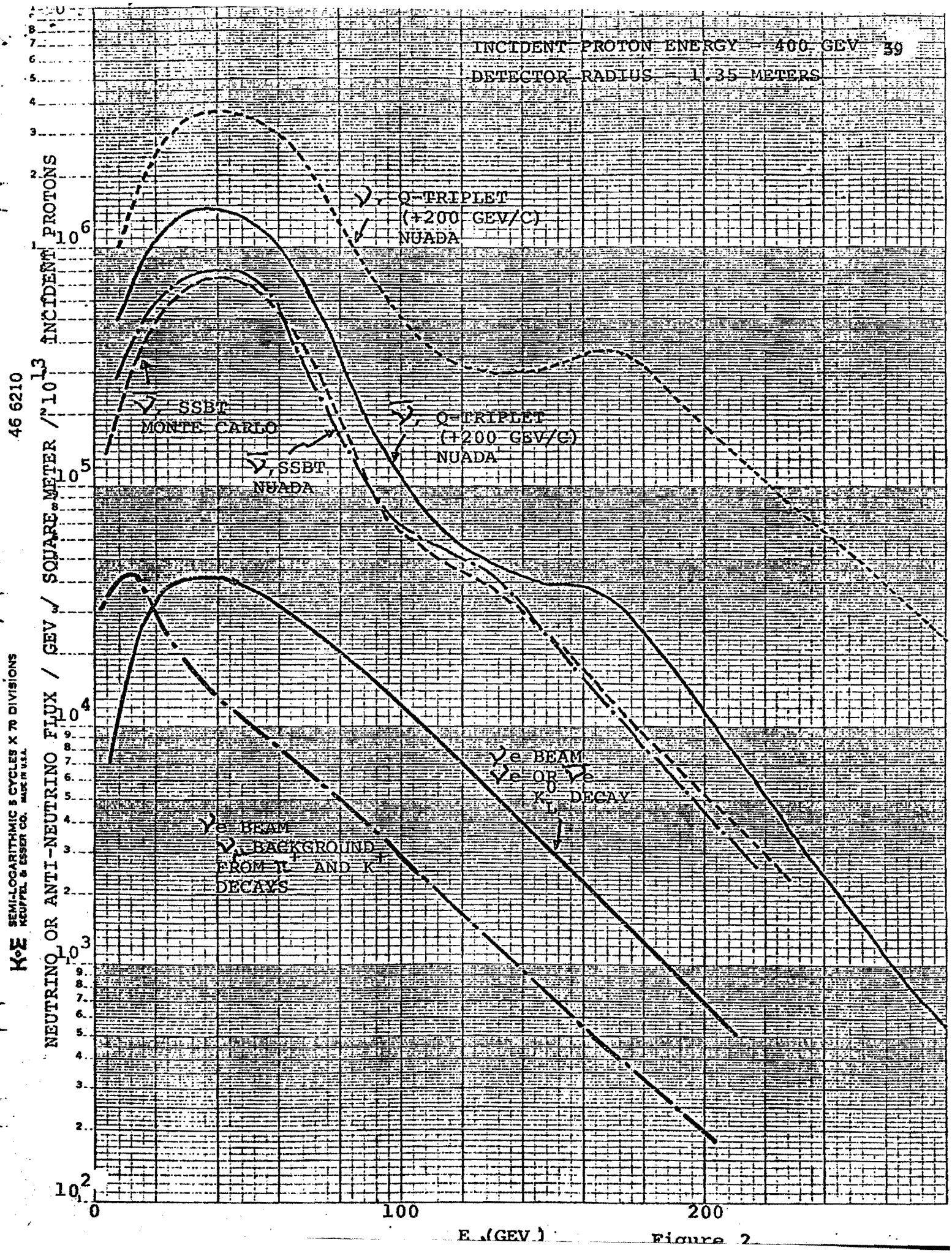
INCIDENT PROTON ENERGY = 400 GEV
DETECTOR RADIUS = 1.35 METERS
ν_μ Q-TRIPLET (+200 GEV/C) NUADA
ν_μ SSBT MONTE CARLO
$\bar{\nu}_\mu$ SSBT NUADA
$\bar{\nu}_\mu$ Q-TRIPLET (+200 GEV/C) NUADA
ν_e BEAM ν_μ BACKGROUND FROM π^+ AND K^+ DECAYS
ν_e BEAM $\bar{\nu}_e$ OR ν_e K_L^0 DECAY
NEUTRINO OR ANTI-NEUTRINO FLUX / GEV / SQUARE METER / 10^{13} INCIDENT PROTONS
10^6
10^5
10^4
10^3
10^2
0
100
200
E_ν (GEV)
46 6210
K&E SEMI-LOGARITHMIC 5 CYCLES X 70 DIVISIONS KEUFFEL & ESSER CO. MADE IN U.S.A.

Figure 2

4-15-77

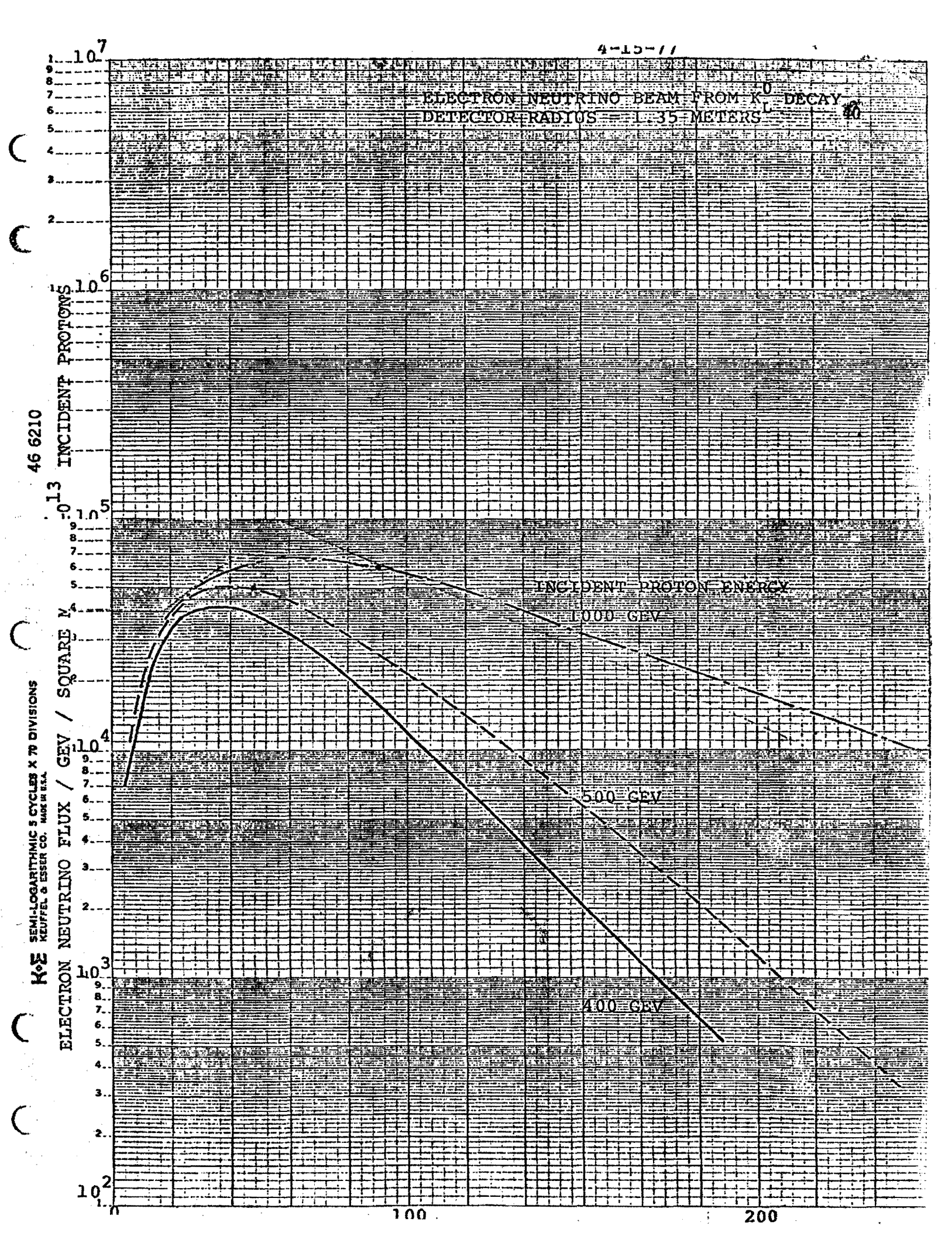

46 6210

K+E SEMI-LOGARITHMIC 5 CYCLES X 70 DIVISIONS
KEUFFEL & ESSER CO. MADE IN U.S.A.